LED COMMUNICATION USING A HIGH SPEED DIGITAL CAMERA

Elam Curry, Javier Perez-Ramirez and **Deva K. Borah**
Advising Professor: Dr. Deva K. Borah, Professor
Klipsch School of Electrical & Computer Engineering
New Mexico State University
Las Cruces, NM 88003, USA
email: mrelam1@nmsu.edu, japera81@gmail.com, dborah@nmsu.edu
Graduate Category

ABSTRACT

An optical communication system using a light-emitting diode (LED) as a transmitter and a high speed digital camera as a receiver is considered. The camera collects data at a rate of 1,200 frames per second (FPS). The pixel values are then processed using equal gain combining (EGC), best pixel selection (BPS), and maximal ratio combining (MRC) techniques. The bit error rate (BER) performance of these techniques is analyzed, and the effect of using different numbers of pixels for receiver processing is considered. The effect of the camera's pixel grid being at an angle with respect to the LED's direct path is experimentally explored.

INTRODUCTION

Optical communication has become a promising technique for providing high speed data rates while maintaining a very secure link [1]. A typical optical communication system consists of optical transmitters, such as laser diodes or LEDs, as well as receivers such as photodiodes or digital cameras. Using a digital camera as a receiver has some advantages over a photodiode, as it allows the transmitter to be moving and provides a much larger field of view for receiving signals. As camera speeds continue to improve, optical communication's potential for high speed data rates will rapidly improve in the future. LEDs operating in the visible light spectral range can serve the dual purpose of lighting a room as well as providing a high speed and secure communication link [2].

One of the challenges facing optical communication is the need to dramatically increase the data rates. One method of achieving this is to use an array of LEDs as a transmitter forming a multiple input multiple output (MIMO) system. The concept of a MIMO optical communication system using LEDs has been demonstrated in [1]. In [3], the BER performance of different diversity combining techniques is compared showing promising results for MRC. An improved receiver processing technique allows lowering of the received optical energy to achieve the same BER performance. As a result, the time duration of the transmitted pulses can be made shorter, which can allow higher data rates. At the same time, LEDs with high data rates must also meet certain room lighting standards. It is shown in [2] that LEDs in a room can maintain International Organization for Standardization (ISO) standards for lighting while also providing a data transmission link, validating the concept of a dual role room light source and communication system.

In this paper, we consider a communication system with an LED as a transmitter and a digital camera as a receiver. We model the received LED image by using the Gaussian mixture model

(GMM) proposed in [3]. While this paper closely follows [3], one of the main contributions of this paper is the results using a high speed complementary metal-oxide semiconductor (CMOS) Promon 501 digital camera from AOS Technologies. Note that the results in [3] were obtained using a Sony charge-coupled device (CCD) digital camera. Accordingly, our results in this paper use 1,200 FPS in contrast to 120 FPS used in [3]. We study three different receiver processing techniques: EGC, BPS, and MRC. EGC's BER performance depends on the number of pixels used. Conditions on how many pixels to use when the receiver uses EGC are given in [3], and the conditions are verified with both simulation and experimental results. As expected, MRC outperforms the other receiver processing techniques in terms of BER performance. We also explore the effect of the LED's angle of incidence on BER performance.

SYSTEM MODEL AND LED/CAMERA PARAMETERS

A single LED is used as a transmitter and a digital camera as a receiver. The camera is positioned so that the tip of the camera lens is at a distance d from the tip of the LED. The camera has a focal length f. In our model, the camera is allowed to rotate by an angle θ relative to being pointed directly at the LED as shown in Fig. 1. In [3], a GMM combined with a reference image pixel

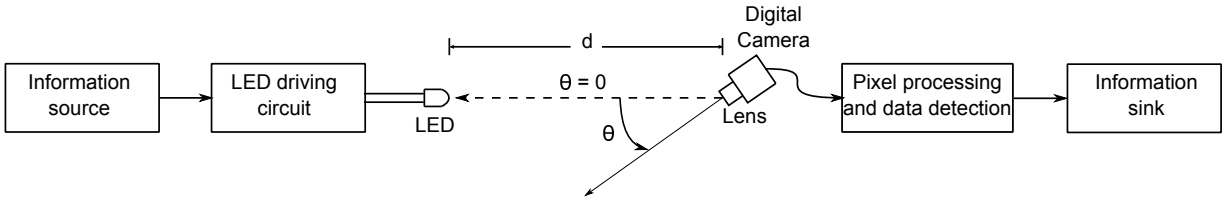

Fig. 1. An optical communication system using a digital camera as a receiver and an LED as a transmitter.

estimation (RIPE) is proposed for the LED image on the camera's pixel plane. Using this model the received signal, $r'_{m,n}$, at the (m,n)th pixel can be expressed as

$$r'_{m,n} = s_{m,n}b + q_{m,n} + n_{m,n} \tag{1}$$

where $s_{m,n}$ is the signal due to the LED in the (m,n)th pixel, $b \in \{0,1\}$ is the transmitted bit, $q_{m,n}$ is the background illumination in the (m,n)th pixel, and $n_{m,n}$ is Gaussian distributed noise in the (m,n)th pixel. The variance of $n_{m,n}$ is given as $\sigma^2_{m,n} = \alpha(s_{m,n}b + q_{m,n}) + \beta$, where α and β are constants [1],[4]. In order to use the GMM proposed in [3], it is necessary to define variables that represent the location of the (m,n)th pixel relative to the pixel that contains the center of the LED image. Let p be the pixel length and g be the gap between pixels. For our camera, $g = 0$ so the pixels are contiguous with no gaps in between. Let the center of the LED image fall at a distance ξ_x in the x direction and ξ_y in the y direction from the center of the (i,j)th pixel, where $-p/2 \leq \xi_x, \xi_y \leq p/2$. Then the location of the center of the (m,n)th pixel can be represented relative to the center of the (i,j)th pixel as $a_x = (m-i)p - \xi_x$ and $a_y = (n-j)p - \xi_y$ as given in [3]. The GMM then gives the signal, $s_{m,n}$, due to the LED at the (m,n)th pixel as

$$s_{m,n} = A(\frac{\mu}{\mu_o})^2 \sum_{k=1}^{\nu} c_k (Q(\frac{a_x - p/2}{\sigma_{x,k}}) - Q(\frac{a_x + p/2}{\sigma_{x,k}})) \times (Q(\frac{a_y - p/2}{\sigma_{y,k}}) - Q(\frac{a_y + p/2}{\sigma_{y,k}})) \tag{2}$$

where $Q(x) = 1/\sqrt{2\pi}\int_x^\infty exp(-y^2/2)dy$, $A = 1/p^2$, μ is the magnification of the LED image and is given as $\mu = f/d$, ν is the number of Gaussian mixture components used to fit the LED image,

$\sigma_{x,k}^2 = (\mu/\mu_o)^2\sigma_k'^2 + \sigma_{b,x}^2$, $\sigma_{y,k}^2 = (\mu/\mu_o)^2\sigma_k'^2 + \sigma_{b,y}^2$, $\sigma_k'^2$ is a constant from GMM fitting, and $\sigma_{b,x}^2$ and $\sigma_{b,y}^2$ are constants due to blur. In our results, we use $\sigma_{b,x} = \sigma_{b,y} = 2.5 \times 10^{-6}$ m.

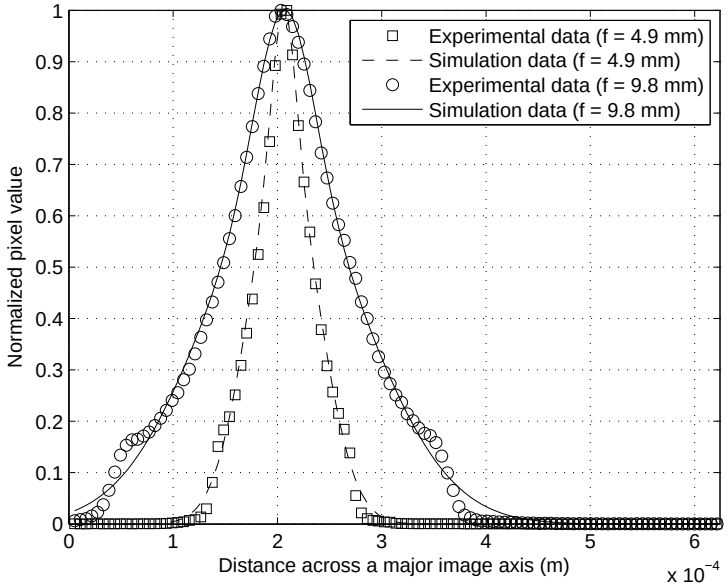

Fig. 2. GMM fit on the received LED image at $d = 10$ cm and $\theta = 0^o$ for $f = 4.9$ mm and $f = 9.8$ mm.

Fig. 2 shows the GMM fit for $s_{m,n}$ with different focal lengths of $f = 4.9$ mm and $f = 9.8$ mm. The normalized pixel value in the figure is defined as $s_{m,n}/s_{max}$, where $s_{max} = \max_{m,n}(s_{m,n})$. The GMM fit uses two Gaussian curves ($\nu = 2$). For the $f = 4.9$ mm fit case, we use $\sigma_1' = 1.0571 \times 10^{-5}$ m, $\sigma_2' = 3.3333 \times 10^{-5}$ m, $c_1 = 5.4438 \times 10^{-8}$, and $c_2 = 1.1261 \times 10^{-6}$, and for the $f = 9.8$ mm fit, we use $\sigma_1' = 2.7181 \times 10^{-5}$ m, $\sigma_2' = 7.9620 \times 10^{-5}$ m, $c_1 = 4.0326 \times 10^{-7}$, and $c_2 = 5.9429 \times 10^{-6}$. The experimental data sets in Fig. 2 are obtained by the digital camera by capturing 10,000 frames with the LED on and 10,000 frames with the LED off. The 10,000 frames with the LED off are then averaged in each pixel to find the average background illumination. The 10,000 frames with the LED on are then averaged in each pixel and the background illumination is subtracted from the averaged frame. Finally, vertical and horizontal lines across the image are considered through the pixel with the highest intensity and the pixel values along these axes are averaged. It can be seen from Fig. 2 that as the focal length increases, the image created by the LED on the pixel plane expands, affecting more pixels.

The noise model for our camera is shown in Fig. 3. The noise variance varies linearly with the pixel values. This plot is generated by averaging each pixel over 10,000 frames and plotting each pixel's variance versus its mean.

EXPERIMENTAL RESULTS AND DISCUSSIONS

Our experiments use a 5 mm super white LED (RL5-W4575) from superbrightleds.com. The digital camera used is an AOS Technologies Promon 501 with a $2/3$ inch pixel grid with 8 bit dynamic range. The camera is capable of resolutions of up to 2048×1088, but in our experiments we use a 320×128 resolution. The sampling rate is 1,200 FPS with an exposure time of 500 μs. The pixel length, p, is 5.5 μm.

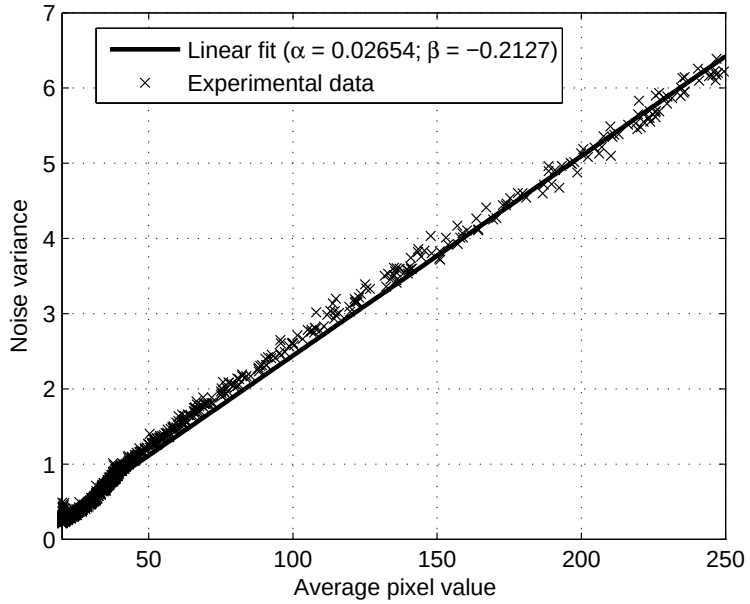

Fig. 3. Linear noise variance model for Promon 501 digital camera from AOS Technologies.

In this paper, three methods for processing the received image are explored: EGC, BPS, and MRC. The background illumination is first removed from the received pixels to create $r_{m,n} = s_{m,n} + n_{m,n}$. Each pixel is multiplied by a weighting factor, $w_{m,n}$, and then summed. In EGC, $w_{m,n} = 1$ for all selected pixels. In BPS, $w_{m,n} = 1$ for the best pixel and $w_{m,n} = 0$ for all other pixels. In MRC, $w_{m,n}$ can be calculated as [3],

$$w_{m,n} = \frac{s_{m,n}}{\frac{1}{2}\alpha s_{m,n} + \alpha q_{m,n} + \beta} \tag{3}$$

For simplicity, in the simulations $q_{m,n}$ is considered to be a constant, q. This value was usually between 15 and 30 in our experiments. The variance of the received pixels with the LED on and with the LED off are given in [3] as $\sigma_{on}^2 = \sum_{m,n} w_{m,n}^2(\alpha(s_{m,n} + q_{m,n}) + \beta)$ and $\sigma_{off}^2 = \sum_{m,n} w_{m,n}^2(\alpha q_{m,n} + \beta)$. The receiver calculates $z_r = \sum_{m,n} w_{m,n} r_{m,n}$ and makes decisions based on a threshold γ_o. Thus, if $z_r > \gamma_o$ then a binary 1 is detected, and a binary 0 is detected otherwise. The decision threshold is given in [3] as $\gamma_o = z_s/(1+\rho)$, where $z_s = \sum_{m,n} w_{m,n}^2 s_{m,n}$ and $\rho = \sigma_{on}/\sigma_{off}$. The expression used to generate analytical results for a given (ξ_x, ξ_y) can be found in [3] as

$$P_b(\xi_x, \xi_y) = \frac{1}{2}(Q(\frac{\gamma_o}{\sigma_{off}}) + Q(\frac{z_s - \gamma_o}{\sigma_{on}})) \tag{4}$$

In order to verify the GMM's representation of the LED's image, the simulation, analytical, and experimental BER results of the three processing schemes are compared for different values of received power, $R = \sum_{m,n} s_{m,n}$, in Fig. 4. The experimental results were obtained by fixing the center of the LED image in the center of a pixel and then capturing 10,000 frames with the LED on and 10,000 frames with the LED off for a given value of R. This was done twice for a total of 40,000 frames for each value of R, and the received power and the BER is averaged over

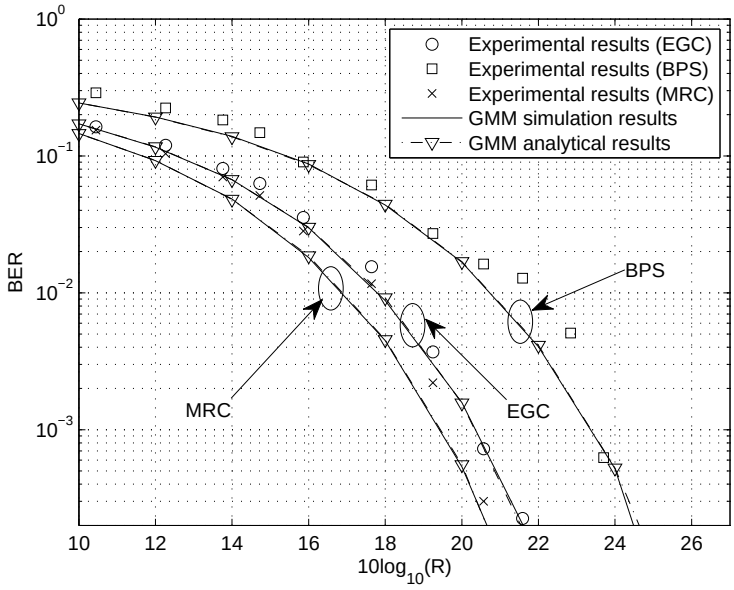

Fig. 4. BER performance at a distance $d = 2$ m, $\theta = 0^o$, and $f = 9.8$ mm. The LED's image is centered in a pixel and kept fixed.

the two sets of data. The 10,000 frames with the LED off are averaged to estimate the average background illumination for each pixel. The 10,000 frames with the LED on are averaged and the average background illumination is removed to estimate z_s, σ^2_{on}, σ^2_{off}, and γ_o for each receiver processing technique, as well as $w_{m,n}$ for MRC. Each individual received image then has the average background illumination removed, and is processed using the three diversity combining methods. For MRC and EGC, we use 9 pixels for data detection. For our results in Fig. 4 we use $d = 2$ m, $\theta = 0^o$, and $f = 9.8$ mm.

It can be seen from Fig. 4 that the experimental results agree well with the analytical and simulation results. MRC and EGC are shown to have similar performance, while the performance of BPS is significantly worse. In the GMM, the shape of the LED image on the camera's pixel plane is controlled by the variance in the x and y directions, $\sigma^2_{x,k}$ and $\sigma^2_{y,k}$. As $\sigma^2_{x,k} = (\mu/\mu_o)^2\sigma^{'2}_k + \sigma^2_{b,x}$ and $\sigma^2_{y,k} = (\mu/\mu_o)^2\sigma^{'2}_k + \sigma^2_{b,y}$ where $\sigma^{'2}_k$, $\sigma^2_{b,x}$, and $\sigma^2_{b,y}$ are constants, the size of the LED image in the x and y direction is controlled by the ratio $(\mu/\mu_o)^2$. Since $\mu = f/d$ and μ_o is a constant, as f increases, the ratio $(\mu/\mu_o)^2$ increases as well. Because of this, the LED's image spreads out as we increase f, effectively lowering the intensity of the central pixel and raising the intensity of the pixels around it. As a result, BPS ignores a large portion of the signal that is present in the pixels surrounding the central pixel. However, EGC and MRC use the surrounding pixels for receiver processing, and as a result they are able to provide much better BER performance. The gap between the BER performance of EGC and MRC demonstrates the improvement in BER performance of MRC obtained by optimally weighting the involved pixels.

The BER performance of EGC significantly depends on the number of pixels used for receiver processing, and the optimal number of pixels to use for EGC can be determined using the conditions given in [3]. Let N be the number of pixels considered, $\tilde{S}_N$ be the sum of pixels considered, and $u_N = 0.5\tilde{S}^2_N/(\frac{\alpha}{2}\tilde{S}_N + \alpha qN + \beta N)$. The conditions state that no further pixels need to be considered for receiver processing once $u_N > u_{N+1}$. In our results, we have found the $s_{m,n}$ values in the decreasing order to be 2.3700, 1.2900, 1.0817, 1.0605, 0.9947, 0.6004, 0.5390,... . Hence $u_5 =$

14.5781 and $u_6 = 14.3138$, so no more pixels need to be considered for receiver processing after $N = 5$ pixels. For MRC it is not necessary to develop such conditions, as the pixel weights, $w_{m,n}$, reduce the effect that low signal pixels have on detection. To validate these results and concepts, the BER performance of EGC and MRC is shown using different number of pixels for receiver processing in Fig. 5. It is apparent from the plot that EGC provides its best BER performance when using $N = 5$ pixels. When the number of selected pixels is small, MRC and EGC show similar performance. However, for a larger number of pixels ($N > 9$), MRC begins to drastically outperform EGC. With $f = 9.8$ mm, the LED image falls in a 5×5 pixel square with the central 3×3 square of pixels receiving the most of the LED's illuminance. Because of this, as more pixels are included in receiver processing, EGC is adding pixels with a lower signal equally, while MRC is applying very small weights to the low signal pixels. The result is that the BER performance of EGC begins to degrade after $u_N > u_{N+1}$, while MRC's BER performance floors, degrading only very slightly in the experimental results.

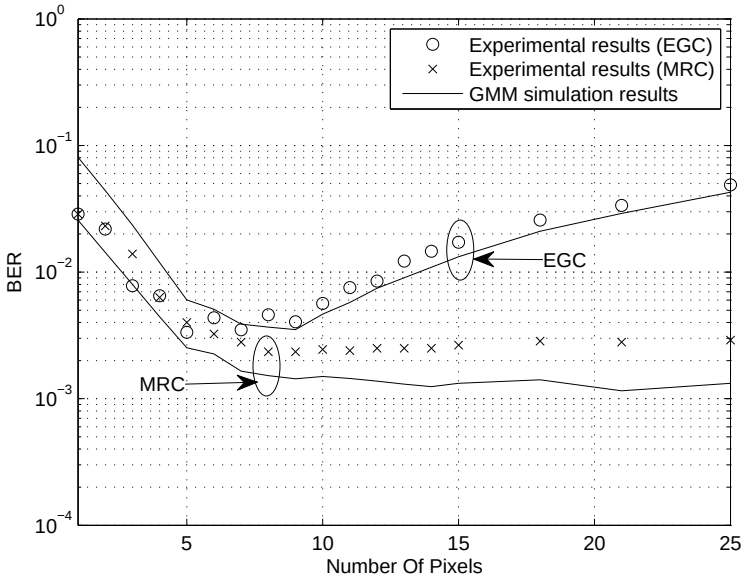

Fig. 5. BER performance at a distance $d = 2$ m, $\theta = 0^0$, and $f = 9.8$ mm using different numbers of pixels. The LED's image is centered in a pixel and kept fixed, and the transmitted power is fixed.

The experimental data in Fig. 5 is obtained using the same method as in Fig. 4. However, only one set of data, consisting of 20,000 frames, is used for the results in Fig. 5. The pixels are placed in a vector in order of descending pixel value, and the N highest intensity pixels are used to generate the results. In our results for Fig. 5, we use a fixed value of $R = 19.0495$, $d = 2$ m, $\theta = 0^o$, and $f = 9.8$ mm.

It is important that an optical communication system is capable of providing reliable data transmission even if the transmitter and receiver are not pointed directly at each other. When using a digital camera as a receiver, the capability of detecting a signal from a transmitter that is at an angle with the camera's pixel plane allows transmitter movement within the camera's field of view. However, the transmitter being somewhere in the camera's field of view other than directly in front of it will cause a loss in signal strength. In Fig. 6, we characterize this loss for different angles of θ along the horizontal axis. Two values of $10log_{10}(R)$ are considered. Our results use up to a maximum horizontal field of view of $\theta = 40^o$. The experimental data in Fig. 6 is obtained by placing the digital

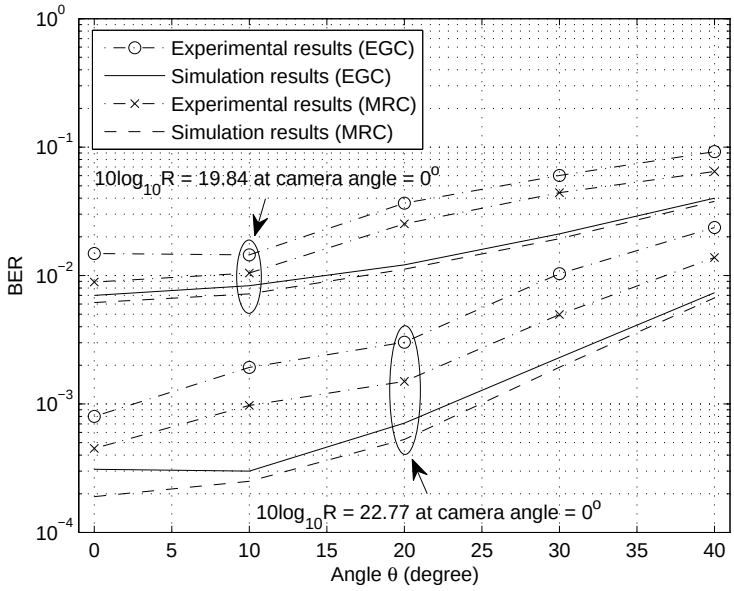

Fig. 6. BER performance at a distance $d = 1$ m, $f = 4.9$ mm for different camera angles θ. BER performance is shown for two fixed values of $10log_{10}(R)$.

camera on a rotatable mount and adjusting the camera viewing angle. This effectively changes the LED's angle of incidence for each value of θ. For each angle θ, the experimental data is obtained by collecting two sets of 20,000 frames, and using the same method as in Fig. 4. In our results for Fig. 6, we use $d = 1$ m and $f = 4.9$ mm.

From Fig. 6, the BER performance of EGC and MRC degrades by a factor of 6.21 and 7.25 respectively at the maximum angle of $\theta = 40^o$ for the case when $10log_{10}R = 19.84$ at $\theta = 0^o$. For the $10log_{10}R = 22.77$ at $\theta = 0^o$ case, the BER performance of EGC and MRC degrades by a factor of 32.88 and 30.73 respectively at the maximum angle of $\theta = 40^o$. The simulation results in Fig. 6 are obtained using (2) with c_k replaced by $c_k \cos\theta$ and using $\sigma^2_{y,k} = (\mu/\mu_o)^2(\sigma'_k/\cos\theta)^2 + \sigma^2_{b,y}$.

CONCLUSION

This paper considers a high speed digital camera as a receiver and an LED as a transmitter in an optical communication system. The camera captures images at a rate of 1,200 FPS. The high speed digital camera used is the Promon 501 from AOS Technologies with a CMOS sensor. The GMM given in [3] is experimentally validated for the high speed camera with a CMOS sensor. Conditions for the number of pixels to use for EGC are explored and are shown to provide optimal performance when satisfied. The loss due to the LED's angle of incidence is experimentally characterized and found to have a significant effect on performance for large camera viewing angles. For small camera viewing angles (e.g., less than 15^o), the BER performance degradation is not significant.

ACKNOWLEDGMENT

This work was partly supported by the National Science Foundation under the Grant ECCS-1202001.

REFERENCES

[1] Hranilovic, S. and Kschischang, F. R., "A pixelated MIMO wireless optical communication system," IEEE Journal of Selected Topics in Quantum Electronics, vol.12, no.4, July-Aug., 2006, pp.859-874.

[2] Komine, T. and Nakagawa, M., "Fundamental analysis for visible-light communication system using LED lights," IEEE Transactions on Consumer Electronics, vol.50, no.1, Feb., 2004, pp.100-107.

[3] Perez-Ramirez, J. and Borah, D. K., "A Single-Input Multiple-Output Optical System for Mobile Communication: Modeling and Validation", IEEE Photonics Technology Letters, vol.26, no.4, Feb., 2014, pp.368-371.

[4] Healey G. E. and Kondepudy R., "Radiometric CCD camera calibration and noise estimation," IEEE Transactions on Pattern Analysis and Machine Intelligence, vol. 16, Mar., 1994, pp. 267-276.